Laboratory Investigation (2020) 100:1388–1399
https://doi.org/10.1038/s41374-020-0474-8

ARTICLE

Early pathogenesis of cystic fibrosis gallbladder disease in a porcine model

Keyan Zarei[1,2] · Mallory R. Stroik[1] · Nick D. Gansemer[1] · Andrew L. Thurman[1] · Lynda S. Ostedgaard[1] · Sarah E. Ernst[1] · Ian M. Thornell[1] · Linda S. Powers[1] · Alejandro A. Pezzulo[1] · David K. Meyerholz[3] · David A. Stoltz[1,2,4]

Received: 30 May 2020 / Revised: 30 June 2020 / Accepted: 7 July 2020 / Published online: 27 July 2020

Abstract

Hepatobiliary disease causes significant morbidity in people with cystic fibrosis (CF), yet this problem remains understudied. We previously found that newborn CF pigs have microgallbladders with significant luminal obstruction in the absence of infection and consistent inflammation. In this study, we sought to better understand the early pathogenesis of CF pig gallbladder disease. We hypothesized that loss of CFTR would impair gallbladder epithelium anion/liquid secretion and increase mucin production. CFTR was expressed apically in non-CF pig gallbladder epithelium but was absent in CF. CF pig gallbladders lacked cAMP-stimulated anion transport. Using a novel gallbladder epithelial organoid model, we found that Cl^- or HCO_3^- was sufficient for non-CF organoid swelling. This response was absent for non-CF organoids in Cl^-/HCO_3^--free conditions and in CF. Single-cell RNA-sequencing revealed a single epithelial cell type in non-CF gallbladders that coexpressed CFTR, MUC5AC, and MUC5B. Despite CF gallbladders having increased luminal MUC5AC and MUC5B accumulation, there was no significant difference in the epithelial expression of gel-forming mucins between non-CF and CF pig gallbladders. In conclusion, these data suggest that loss of CFTR-mediated anion transport and fluid secretion contribute to microgallbladder development and luminal mucus accumulation in CF.

Introduction

Cystic fibrosis (CF) is a life-shortening disease with significant healthcare costs, affecting about 70,000 people worldwide [1]. Mutations in the gene encoding the CF transmembrane conductance regulator (CFTR), an anion channel, lead to multiorgan system disease including the hepatobiliary system [2]. CF hepatobiliary disease represents the third leading cause of death for people with CF [3–5]. Diagnosis of CF hepatobiliary disease is complicated due to variability of disease forms; it is also unclear why only a fraction of individuals with CF develop hepatobiliary disease [6–9]. While CFTR modulators are efficacious in individuals with certain *CFTR* mutations, these therapies do not benefit all patients and they are not a cure [10]. Thus, there is a need to better understand CF hepatobiliary disease pathogenesis.

CFTR is expressed in the gallbladder and this organ can be used to better understand the role of CFTR in the extrahepatic biliary tract [11, 12]. The gallbladder stores, concentrates, and modifies bile. Gallbladder disease exists

Supplementary information The online version of this article (https://doi.org/10.1038/s41374-020-0474-8) contains supplementary material, which is available to authorized users.

✉ David K. Meyerholz
david-meyerholz@uiowa.edu

✉ David A. Stoltz
david-stoltz@uiowa.edu

1 Department of Internal Medicine and Pappajohn Biomedical Institute, Roy J. and Lucille A. Carver College of Medicine, University of Iowa, Iowa City, IA 52242, USA

2 Department of Biomedical Engineering, University of Iowa, Iowa City, IA 52242, USA

3 Department of Pathology, Roy J. and Lucille A. Carver College of Medicine, University of Iowa, Iowa City, IA 52242, USA

4 Department of Molecular Physiology and Biophysics, Roy J. and Lucille A. Carver College of Medicine, University of Iowa, Iowa City, IA 52242, USA

in up to 30% of individuals with CF [13, 14]. Potential forms of CF gallbladder disease include cholelithiaisis, cholecystitis and a small gallbladder (microgallblader) [15, 16]. Interestingly, gallbladder CFTR expression is high relative to other tissues in humans [17, 18]. However, the exact function of CFTR in the gallbladder is unclear. In studies with human and murine gallbladder tissue, CFTR activation leads to greater anion secretion in non-CF versus CF mucosa [19–21]. *CFTR*$^{-/-}$ mice have more acidic gallbladder bile and demonstrate defective gallbladder emptying relative to wild-type controls [22]. These models have certain limitations. For example, when studying human surgical tissue samples, patients are frequently older and have advanced disease complicating the study of the onset of CF disease [11, 19, 20]. CF mouse models do not demonstrate a phenotype resembling human CF biliary disease, limiting the translational impact of pathogenesis studies [22, 23].

The CF pig model recapitulates human CF disease and allows for assessing CF pathogenesis at birth [24, 25]. Newborn CF pigs demonstrate a microgallbladder [26]. CF pigs also have decreased bile volume secretion and a more acidic gallbladder bile pH, consistent with defective CFTR function [27]. Luminal obstruction is also found in the newborn CF pig gallbladder, although the composition of this obstructing material is unknown [26]. In contrast to CF pig airway disease, the gallbladder phenotype develops in the absence of infection or consistent inflammation [26, 28] and the underlying pathogenesis is not yet clear. Thus, the CF pig gallbladder represents a model to study CF mucus pathogenesis in the absence of infection and inflammation.

In this study, we investigated gallbladder disease in the newborn CF pig (i.e., in the first 24 h of life), focusing on the role of CFTR in gallbladder epithelial anion and fluid secretion and the development of the mucus phenotype. We hypothesized that CFTR loss in the newborn pig gallbladder impairs Cl^-/HCO_3^- transport and fluid secretion and enhances mucin production.

Methods

CF pig model

The development of the CF pig model has been previously reported [24]. Animals were purchased from Exemplar Genetics (Sioux City, IA). All protocols were approved by the University of Iowa Institutional Animal Care and Use Committee. Newborn (within the first 24 h of life) *CFTR*$^{+/+}$ and *CFTR*$^{-/-}$ pigs (henceforth referred to as non-CF and CF pigs respectively) were sedated with ketamine/xylazine (Akorn) and euthanized with phenobarbital sodium/phenytoin sodium (Euthasol; Virbac).

Immunohistochemistry and quantitative histology

Immunohistochemistry studies were done by the University of Iowa Comparative Pathology Laboratory [29]. Briefly, gallbladders from newborn piglets were excised and fixed in 10% normal-buffered formalin (room temperature, 1 h). Tissues were embedded in paraffin, serially sectioned using a microtome (~4 µm) and hydrated through a sequence of xylene/alcohol baths. Subsequently, antigen retrieval was done using the NxGen Decloaking Chamber™ (Biocare Medical) with a citrate buffer (pH 6.0, 110 °C, 15 min). Endogenous peroxidase activity was quenched (hydrogen peroxide 3%, 8 min), endogenous avidin/biotin was blocked (Avidin/Biotin Blocking Kit, Vector Laboratories, Inc.) and nonspecific background was blocked (equine serum, 5% in 1x Dako Buffer). CFTR immunohistochemistry was done with mouse anti-CFTR 769 (1:1200, 60 min; CFF/UNC), generously supplied by Dr. John Riordan, University of North Carolina—Chapel Hill and the Cystic Fibrosis Foundation Therapeutics. MUC5AC and MUC5B immunohistochemistry reagents were mouse anti-MUC5AC (clone 45M1) monoclonal (1:75, 30 min; Novus Biologicals) and anti-MUC5B polyclonal (1:60,000, 30 min; LifeSpan BioSciences) respectively. Secondary Ab (1:200, 30 min; Vector Biotinylated Anti-Mouse IgG) was then applied followed by Vector ABC Reagent (30 min, Standard VECTASTAIN® Elite® ABC Kit, Vector Laboratories, Inc.) and chromogen (room temperature, DAB plus for 5 min followed by DAB Enhancer for 3 min). Tissues were counterstained with Harris hematoxylin (1 min, Surgipath, Leica Microsystems, Inc.). Slides were blued in Scott's Tap water, dehydrated through a sequence of alcohol/xylene baths and subsequently coverslipped. For quantitative mucin histology, high resolution images of the slides were acquired with the ×20 objective at 0.24 µm/pixel resolution by the Panoramic 1000 slide scanner (3DHISTECH). Gallbladder tissue sections were visualized using the 3DHISTECH CaseViewer software (3DHISTECH) to quantify histological features of all tissue specimens. Area quantifications of mucin-positive regions of images was done through the Fiji software. Briefly, an image mask for the gallbladder epithelium was traced, the image was thresholded, and the percentage of thresholded area relative to mask area was calculated. As a positive control for MUC5AC and MUC5B, newborn non-CF pig airways were also sectioned and stained in parallel; thresholding settings were optimized and established from positive tissue controls.

CFTR immunocytochemistry

Gallbladders from newborn piglets were excised, placed in ice-cold 30% sucrose solution, quick frozen with liquid nitrogen in optical cutting temperature compound, and stored at −80 °C. Frozen tissue was then sectioned using a Cryostat microtome (7 µm sections), fixed in 4% formaldehyde (room temperature, 15 min), permeabilized with 0.2% Triton X-100 (Thermo Fisher; room temperature, 20 min) and blocked in Superblock (Thermo Fisher) supplemented with 5% filtered normal goat serum (Jackson Immunologicals; room temperature, 1 h). Sections were then immunostained with rabbit anti-β-ZO-1 (1:100; Zymed) and mouse anti-CFTR 596 (1:100, CFF/UNC) for 2 h at 37 °C. Subsequently, the sections were incubated in goat anti-mouse Alexa Fluor 488 (1:1000; Molecular Probes) and goat anti-rabbit Alexa Fluor 568 (1:1000; Molecular Probes/Invitrogen), mounted in Vectashield plus DAPI (Vector Labs), and visualized using an Olympus Fluoview FV1000 confocal microscope.

Ussing chamber studies

Gallbladders were separated from the liver parenchyma, a longitudinal cut was made along the surface of the gallbladder exposing the lumen, and a 3 mm × 3 mm square section was excised, mounted in Ussing chambers (Physiologic Instruments), and bathed in a Krebs–Ringer solution (144 mM NaCl, 25 mM HCO_3, 1.2 mM $CaCl_2$, 1.2 mM $MgCl_2$, 2.4 mm K_2HPO_4, 0.6 mm KH_2PO_4, 5 mM dextrose in 5% CO_2 (vol/vol), pH = 7.4) on both the apical and basolateral sides, as previously described [30]. The final concentrations of the chemicals were the following: forskolin (apical—10 µM), 3-isobutyl-2-methylxanthine (IBMX) (apical—100 µM), GlyH (apical—100 µM), 4,4′-diisothiocyanostilbene-2,2′-disulfonic acid (DIDS) (apical—100 µM), and bumetanide (basolateral—100 µM).

Development of porcine gallbladder organoid model

Methodology for the organoid model was adapted from a published protocol for human gallbladder tissue [31]. The gallbladder and cystic duct were separated from the liver parenchyma, a longitudinal incision was made along the gallbladder to expose its lumen, and the excised tissue was placed in cold William's E media supplemented with nicotinamide (10 mM), sodium bicarbonate (17 mM), 2-phospho-L-ascorbic acid trisodium (0.2 mM), sodium pyruvate (6.3 mM), glucose (14 mM), HEPES (20 mM), dexamethasone (100 nM), insulin–transferrin–selenous acid premix (1:100), and penicillin–streptomycin (100 U/mL; 100 µg/mL). The pig gallbladder tissue was minced using sterile scalpels and digested for 2 h at 37 °C in William's E media containing collagenase (Sigma-Aldrich, 10 mg/mL). After incubation, 2% by volume fetal bovine serum was added to neutralize the collagenase and the cell suspension was filtered over a 100 µm filter. Cells were centrifuged down at 440 × *g* for 5 min. The cell pellet was washed with supplemented William's E media and centrifuged down again at 440 × *g* for 5 min. The resulting cell pellet was resuspended in supplemented William's E media containing the following growth factors: 500 ng/mL human recombinant R-spondin 1 (R&D) and 40 ng/mL human epidermal growth factor (R&D). These growth factor-containing media are referred to as gallbladder organoid media. For the initial plating of the cells, 10 µM Y-27632 dihydrochloride (Tocris) was also added to the media but was not included for subsequent media changes. The cell pellet was mechanically dissociated so that there were cell clusters of ~10–20 cells. Two parts by volume Matrigel (Corning) was added to the cell suspension and the final mixture was plated in prewarmed 24-well culture plates in small, 5–10 µL drops (35 µL per well). The plates were inverted and incubated for 10–20 min at room temperature, and then for another 30–40 min at 37 °C. Overall, 400 µL of prewarmed gallbladder organoid media was then added to each well. Media were changed every 3–4 days. Organoids were passaged approximately once per month: organoids were mechanically dissociated from Matrigel using cold William's E media, centrifuged at 440 × *g* for 5 min, and replated at a dilution of 1:5.

Organoid swelling assay

All experiments were done on the Zeiss LSM-880 multiphoton with temperature control (37 °C) and humidity chamber. All experiments were done with passage 0 or 1 organoids. Non-CF and CF pig organoids were plated in 24-well culture dishes 3–4 days prior to imaging. Approximately 30 min prior to the experiment, media were aspirated and replaced with Krebs–Ringer solution (118.9 mM NaCl, 25 mM $NaHCO_3$, 1.2 mM $CaCl_2$, 1.2 mM $MgCl_2$, 2.4 mm K_2HPO_4, 0.6 mm KH_2PO_4, 5 mM dextrose in 5% CO_2 (vol/vol), pH = 7.4), Cl^--free ringer solution (118.9 mM sodium gluconate, 25 mM $NaHCO_3$, 2.4 mm K_2HPO_4, 0.6 mm KH_2PO_4, 5 mM calcium gluconate, 1 mM magnesium gluconate, 5 mM dextrose in 5% CO_2 (vol/vol), pH = 7.4), HCO_3^--free Ringer's solution (135 mM NaCl, 1.2 mM $CaCl_2$, 1.2 mM $MgCl_2$, 2.4 mm K_2HPO_4, 0.6 mm KH_2PO_4, 5 mM HEPES, 5 mM dextrose, pH = 7.4), or Cl^--free and HCO_3^--free Ringer's (143.9 mM sodium gluconate, 2.4 mm K_2HPO_4, 0.6 mm KH_2PO_4, 5 mM calcium gluconate, 1 mM magnesium gluconate, 5 mM dextrose, pH = 7.4). Baseline

measurements of 5–10 organoids per condition were obtained. Forskolin (final concentration—10 μM) was added to the Ringer's solution and organoids were monitored for 1 h with an image acquisition interval of 5 min. Whole organoid areas were obtained by hand tracing the images in Fiji.

Organoid immunocytochemistry

Pig gallbladder organoids were mechanically dissociated from the Matrigel, washed, and fixed in 4% PFA for 15 min at 4 °C. Organoids were kept in suspension at 4 °C while they were permeabilized in 0.3% Triton for 1 h, and blocked in Superblock (Thermo Fisher) with 4% normal goat serum for 48 h. Organoids were then incubated with primary antibodies overnight: mouse anti-CFTR (clone 769) (1:100 dilution, University of North Carolina—Chapel Hill and the Cystic Fibrosis Foundation Therapeutics) and rabbit anti-Na^+/K^+-ATPase (clone EP1845Y) (1:100 dilution, Abcam). Organoids were then washed with PBS and incubated with goat anti-mouse and goat anti-rabbit secondary antibodies conjugated to Alexa Fluor 488 and Alexa Fluor 568 (1:1000; Molecular Probes/Invitrogen), respectively. Organoids were washed again with PBS. Organoids were then incubated with Alexa Fluor 633 conjugated phalloidin (1:40; Molecular Probes/Invitrogen) for 1 h at room temperature. Organoids were then washed in PBS, mounted with Vectashield plus DAPI (Vector Labs), coverslipped, and visualized with an Olympus Fluoview FV1000 confocal microscope 60x oil lens.

Real-time quantitative polymerase chain reaction (qRT-PCR)

Total RNA was isolated from whole gallbladder using a RNeasy Lipid Tissue Kit (Qiagen) according to the manufacturer's instructions. cDNA was amplified using the 7900HT Fast Real-Time PCR System (Applied Biosystems). qPCR was performed using the Takara Bio SYBR Green Master Mix including ROX (Clontech). Gene expression relative to the beta actin housekeeping gene was performed using the ΔΔCT method. Primer sequences for the genes assayed in this experiment are as follows: *β-actin* forward CTGCGGCATCCACGAAACT, *β-actin* reverse GTGATCTCCTTCTGCATCCTGTC; *CFTR* forward CAC TACGCTGGTTCCAAATGC, *CFTR* reverse ATCCCAAC TGTTCCTTCTCCTTC.

Bulk RNA-sequencing

Total RNA was isolated from whole gallbladder using a RNeasy Lipid Tissue Kit (Qiagen) according to the manufacturer's instructions. Genomic DNA was digested using DNase I (Qiagen). RNA samples were then quantified using fluorimetry (Qubit 2.0 fluorometer; Life Technologies), and RNA quality was assessed using an Agilent BioAnalyzer 2100 (Agilent Technologies). Only samples with RNA integrity numbers > 9 were used. Samples were then processed and sequenced at the Genomic Division of the Iowa Institute of Human Genetics. Ribosomal RNA was depleted using the Ribo Zero Gold kit (Illumina). Sample libraries were prepared using standard Illumina protocol with the TruSeq Stranded Total RNA kit (Illumina). Sequencing was done on the Illumina Hiseq 4000 (Illumina) across 2 lanes with 150 base paired-end reads. FastQC (version 0.11.9) was used to verify the quality of the reads. Raw reads were pseudoaligned using *Sus scrofa* reference genome 11.1 and quantified using Kallisto (version 0.45.0) with 100 bootstraps [32], and gene-level differential expression analysis was performed using Sleuth (version 0.30.0) [33]. Confidence intervals for fold changes were calculated using DESeq2 (version 1.28.1) [34]. Differentially expressed genes were assessed by having a q-value less than 0.05; genes meeting this criteria were input into the Ingenuity Pathway Analysis (Qiagen Inc.) and Enrichr [35, 36] for pathway and gene ontology biological process analyses, respectively.

Data records

Data have been deposited in the National Center for Biotechnology Information and are accessible through the GEO Series accession number GSE152145.

Single-cell RNA-sequencing

Whole gallbladder from a non-CF pig was excised and cut open to reveal the lumen. The outermost layer of cells facing the lumen were mechanically scraped into DPBS-DTT. Cells were dissociated for 1 h in 1.4 mg/mL pronase and 40 U DNase, and then filtered through a 40 μm tissue strainer. Density gradient centrifugation was performed with Iodixanol (OptiPrep) to separate live and dead cells. Cells were stained with trypan blue, counted using a hemocytometer, and submitted for sequencing in DPBS with 0.04% BSA. Libraries were prepared by the Iowa Institute of Human Genetics-Genomics Division core facility at the University of Iowa using the Chromium Single-Cell 3′ Reagent Kit v3 Chemistry (10x Genomics) and sequenced on the HiSeq 4000 Sequencing System (Illumina). Single-cell RNA-sequencing data were assessed for quality using FastQC (version 0.11.9), preprocessed using CellRanger (version 3.0.02), aligned using STAR (version 2.7.3) [37], analyzed using Seurat

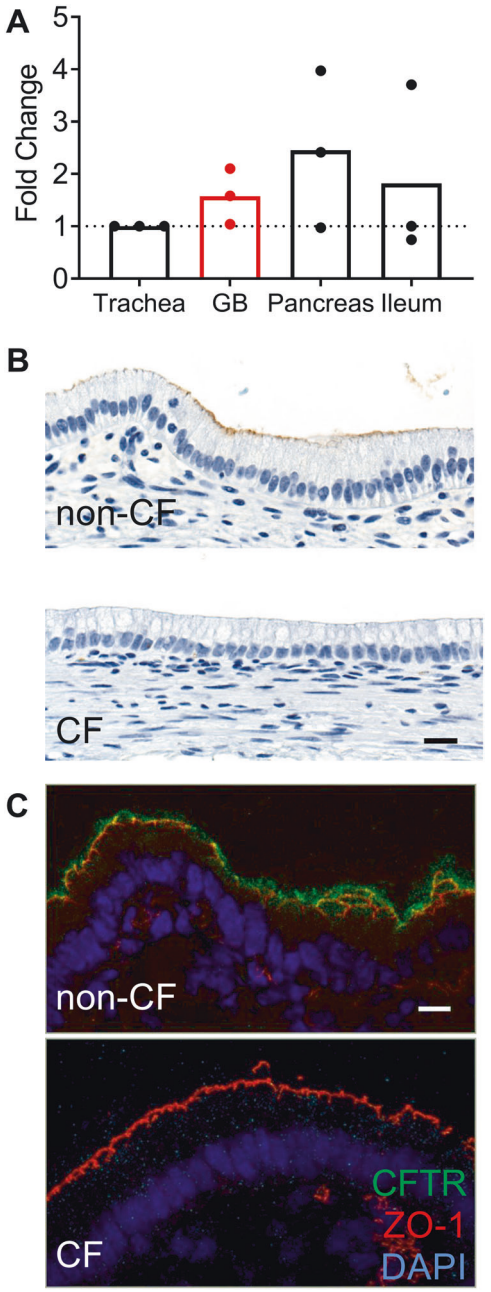

Fig. 1 The newborn pig gallbladder epithelium expresses apical CFTR. a qRT-PCR-determined *CFTR* expression in newborn non-CF pig tissue samples. Data are relative to tracheal *CFTR* expression. Each symbol represents a different animal. The *y*-axis is the fold change calculated using the following-equation: fold change $= 2^{-\Delta\Delta CT}$ where ΔCT is the difference between the CT value for CFTR and the housekeeping gene, β-actin, and ΔΔCT represents the difference between the ΔCT values for the tissue of interest normalized to tracheal expression. **b**, **c** Apical CFTR in newborn gallbladder detected by immunohistochemistry (brown, **b**) and immunocytochemistry (green, **c**) for non-CF and CF, top and bottom, respectively, (scale bar = 10 μm).

(version 3.0) [38, 39], and visualized in the Loupe Cell Browser (10x genomics).

Statistics

All statistics were conducted by Graphpad Prism software unless stated otherwise. Non-parametric *t*-tests (Mann–Whitney) or one-way ANOVA analyses were conducted when appropriate. $P < 0.05$ was considered statistically significant.

Results

Newborn pig gallbladder epithelia express CFTR

Earlier studies identified CFTR in the biliary tract epithelium [11, 40]. To quantify CFTR levels in porcine gallbladder epithelium, we first measured *CFTR* mRNA using qRT-PCR. Newborn pig gallbladder expressed *CFTR* at levels similar to other tissues (Fig. 1a). Both immunohistochemical and immunocytochemical studies of newborn non-CF pig gallbladder revealed a uniform, simple columnar epithelium with apical CFTR expression on nearly every cell (Fig. 1b, c). In contrast, using similar methodology, we previously found that CFTR only localized to a subset of airway epithelial cells [24]. Newborn CF pig gallbladder epithelium lacked CFTR staining (Fig. 1b, c).

CF pig gallbladders lack CFTR-mediated electrolyte transport

To investigate the role of CFTR in gallbladder epithelial electrolyte transport, we mounted non-CF and CF gallbladder tissue in Ussing chambers and assayed transepithelial current. Basal short-circuit current (I_{sc}) was higher in non-CF than CF gallbladder tissue (Fig. 2a). Forskolin and IBMX, which lead to CFTR activation, increased I_{sc} in non-CF but not CF gallbladders (Fig. 2a, b). GlyH-101, a CFTR inhibitor, decreased I_{sc} in non-CF tissues, but had no effect in CF. Subsequent addition of apical DIDS, to block non-CFTR Cl^- channels, and basolateral bumetanide, which inhibits the Na^+–K^+–$2Cl^-$ cotransporter, caused minimal I_{sc} changes in either genotype (Fig. 2a, b). These data suggest that CFTR is a major contributor to anion transport in newborn pig gallbladder tissues.

CF pig gallbladder epithelial organoids do not swell

Given the defects in anion transport, we hypothesized that epithelial fluid transport would be defective in the CF pig gallbladder. Decreased fluid secretion by the biliary epithelium could explain the small gallbladder (microgallbladder) and decreased bile output into the duodenum observed in the CF pig [27]. To investigate the role of CFTR in gallbladder fluid secretion, we created non-CF and

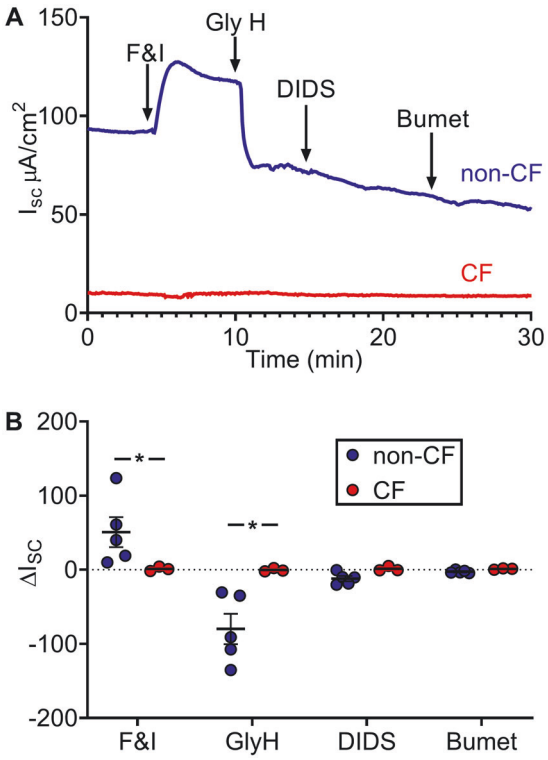

Fig. 2 Newborn CF pig gallbladder tissue lack CFTR-mediated anion transport. a Representative traces from non-CF (blue) and CF (red) freshly excised newborn pig gallbladders mounted in Ussing chambers for electrophysiological studies. The following agents were added sequentially: apical 10 µM forskolin/100 µM IBMX (F&I), apical 100 µM GlyH-101, apical 100 µM DIDS, and basolateral 100 µM bumetanide (Bumet). **b** Changes in I_{sc} (ΔI_{sc}) values from freshly excised gallbladder tissue from five non-CF and three CF animals. Bars represent mean ± SEM. Asterisk (*) indicates $p < 0.05$.

CF pig gallbladder organoids based upon work by Sampaziotis et al. [31]. Pig gallbladder organoids formed within 3–4 days. Non-CF organoids consistently developed a central lumen surrounded by a layer of epithelial cells (Fig. 3a). CF pig gallbladder organoids were smaller than non-CF (Fig. 3a, b) and had a variety of morphologies, frequently demonstrating smaller lumens and a "budding" phenotype with multiple luminal spaces. Regardless, apical actin and basolateral Na^+/K^+-ATPase staining demonstrated that both non-CF and CF organoids formed with the apical epithelial surface facing the organoid lumen (Fig. 3c). Similar to our tissue studies, nearly every cell in non-CF organoids expressed apical CFTR whereas there was no staining in CF organoids (Fig. 3c). To assess fluid secretion in the organoid model, non-CF and CF pig gallbladder epithelial organoids were treated with forskolin. CFTR activation in non-CF organoids caused swelling (Video S1), while this response was completely absent in CF pig organoids (Video S2 and Fig. 3d, e).

Studies have demonstrated important roles for both Cl^- and HCO_3^- transport by CFTR [41–49]. Therefore, we determined the individual and combined contribution(s) of these two anions to gallbladder epithelial fluid secretion. Conditions lacking either Cl^- or HCO_3^- maintained the swelling response seen when both anions were present. Only in the absence of both Cl^- and HCO_3^- did non-CF organoids fail to swell (Fig. 3e).

Gallbladder epithelial cells coexpress CFTR, MUC5AC, and MUC5B

Mucus changes are a common feature in CF. The gallbladder also expresses several gel-forming mucins (MUC2, MUC5AC, MUC5B, and MUC6) [50–53]. Thus, we investigated the expression of these mucins within the pig gallbladder epithelium. We conducted single-cell RNA-sequencing of the non-CF pig gallbladder. The epithelial cell population, identified by epithelial cell adhesion molecule (*EPCAM*) (Fig. S1), demonstrated high expression of *MUC5AC*, *MUC5B*, and *CFTR* in the same cell population (Fig. 4). *MUC2* and *MUC6* were expressed at very low levels. These findings suggest that nearly all gallbladder epithelial cells coexpress *CFTR*, *MUC5AC*, and *MUC5B*. Consistent with previous studies in the gallbladder and cholangiocytes, we also found that these cells express genes related to ion and fluid transport (*SLC4A2*, *ANO1*, *SLC9A3*, and *AQP1*) [54–57], receptor signaling (*SCTR*, *VIPR1*, *P2RY2*, and *TLR4*) [58–61], and bile and cholesterol transport (*ABCC3*, *SLC51A*, *ABCB4*, and *ABCC4*) [62–65] (Fig. S1).

Non-CF and CF pig gallbladder transcriptional profiles are similar despite CF gallbladder remodeling

Since gallbladder disease is present in the CF pig at birth and mucus accumulation associates with CF disease in other organs, we determined if CFTR loss in the newborn pig gallbladder induced transcriptional changes or altered mucin gene expression. RNA-sequencing revealed, surprisingly, that only 163 genes were differentially expressed between non-CF and CF pig gallbladders (Fig. 5a and Supplementary Table 1). Gene ontology analysis of these differentially expressed genes indicated that several pathways were altered in CF including mitochondrial function, the unfolded protein response, and NRF-2 mediated oxidative stress response (Fig. 5b, c). Similar to the single-cell RNA-sequencing data, the predominant gel-forming mucins expressed were *MUC5AC* and *MUC5B*, while *MUC2* and *MUC6* had extremely low normalized transcript counts (Table 1). There was no differential expression, between non-CF and CF, for *MUC2*, *MUC5AC*, *MUC5B*, or *MUC6* after adjusting for multiple testing. These findings suggest that despite

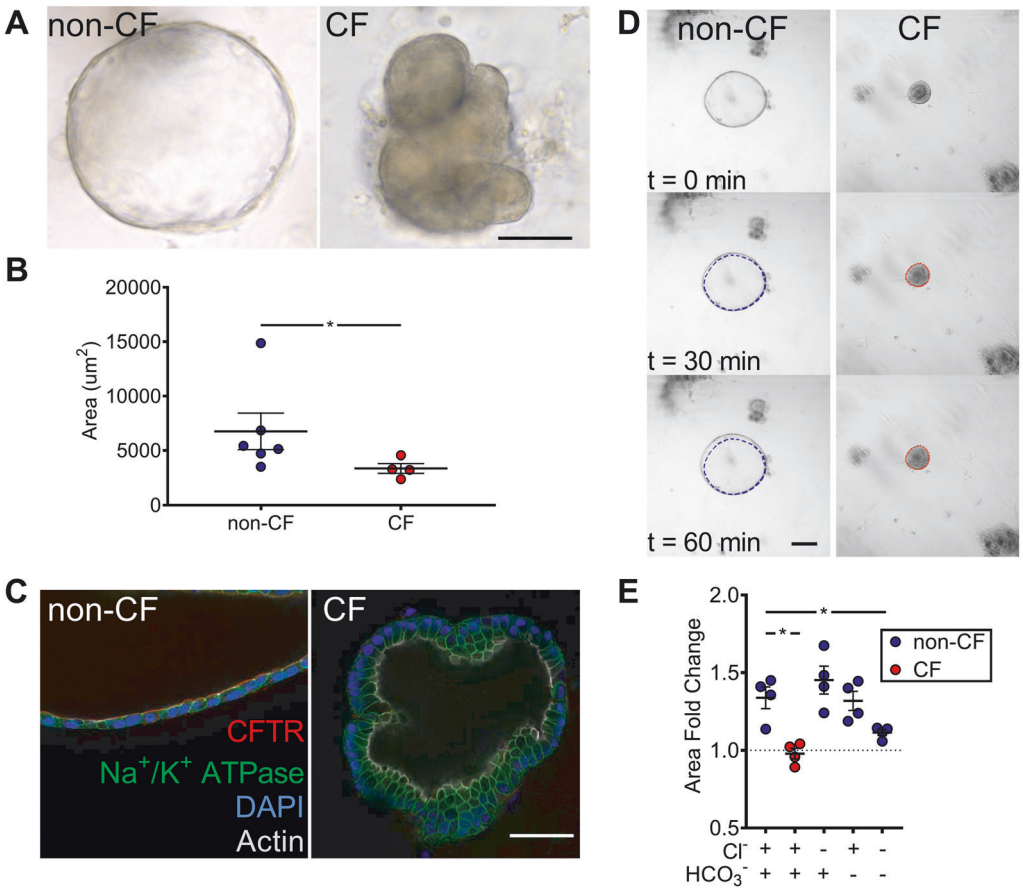

Fig. 3 CF pig gallbladder organoids lack swelling response. **a** Brightfield images of non-CF and CF organoids (scale bar = 100 µm). **b** Whole organoid area measurements at baseline. **c** Immunocytochemistry of non-CF and CF organoids (scale bar = 50 µm). **d** Representative images of non-CF and CF forskolin-induced organoid swelling over time (0, 30, and 60 min). Dashed lines denote starting area. **e** Fold change of whole organoid area post incubation in 10 µM forskolin for 1 h. Values are normalized to organoid response to vehicle (DMSO) in the same conditions. Bars represent mean ± SEM. Each symbol represents data from a different animal. Asterisk (*) indicates $p < 0.05$.

significant gallbladder remodeling in CF, there are minimal transcriptional changes associated with CFTR loss, including mucin transcript expression.

CF pig gallbladders have increased luminal MUC5AC and 5B accumulation

We were surprised to find that the CF pig gallbladder had minimal changes in mucin transcription since our earlier work found significant luminal obstruction in the newborn CF pig gallbladder [24, 26]. To further investigate the mucus phenotype, we performed mucin staining in non-CF and CF gallbladders. Given the low transcriptional expression of MUC2 and MUC6 in the porcine gallbladder, we focused on MUC5AC and MUC5B. All newborn non-CF pig gallbladder lumens were free of MUC5AC- and MUC5B-positive material (Fig. 6a and Table 2). CF pig gallbladders consistently demonstrated luminal accumulation of MUC5AC and MUC5B (Fig. 6a and Table 2), despite lacking significant inflammation [26] or infection (Supplementary Table 2). To determine if the luminal mucus changes correlated with epithelial mucus changes, we performed quantitative histological analyses of non-CF and CF newborn pig gallbladder epithelium (Fig. 6a). In both non-CF and CF, mucin staining was variable between tissue samples, but MUC5B was the predominant gel-forming mucin. Epithelial MUC5AC and MUC5B staining were similar between non-CF and CF. (Fig. 6b, c). Taken with our transcriptional studies, these results suggest that the mucus obstructing the CF pig gallbladder is due to accumulation rather than overproduction.

Discussion

We previously found that at birth, CF pigs have a small gallbladder with luminal obstruction [24, 26, 28]. This study expands on our earlier work demonstrating that CFTR

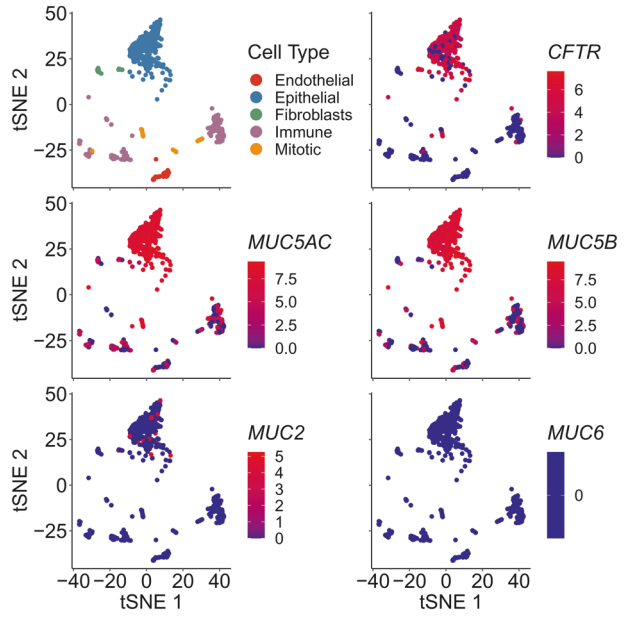

Fig. 4 Single-cell RNA-sequencing demonstrates a single population of gallbladder epithelial cells expressing CFTR. t-SNE plots of single-cell RNA-sequencing. Different cell types collected from luminal scraping of the gallbladder epithelium. Each symbol correlates to a single cell while the coloring of each cell represents the cell type grouping (indicated by the text in the same color). CFTR expression correlates with epithelial cells. MUC5AC and MUC5B were highly expressed in the same epithelial cells expressing CFTR. MUC2 and MUC6 were not highly expressed in the epithelial cell population. Each symbol represents a single cell and the hue of each symbol represents the expression level for that gene.

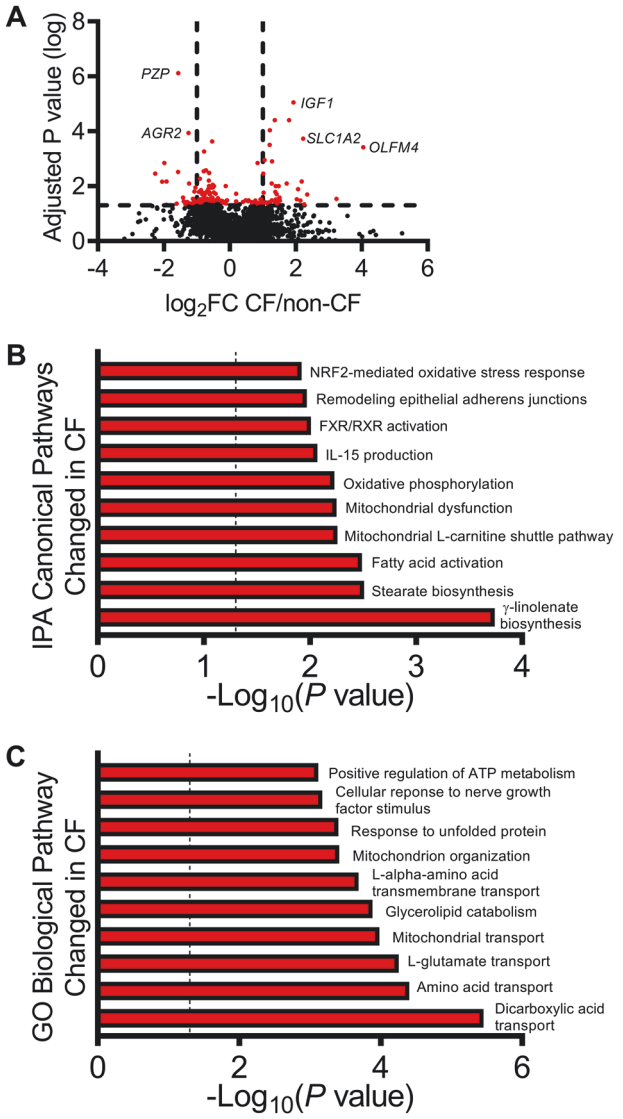

Fig. 5 Newborn CF pig gallbladders demonstrate limited transcriptional changes compared to non-CF. a Volcano plot showing differential gene expression between CF and non-CF newborn pig gallbladder. The *y*-axis represents the logarithm of the *p* value adjusted for the false-discovery rate. Some of the top differentially expressed genes (smallest adjusted *p* value) are labeled for reference. **b** Canonical Pathways from Ingenuity Pathway Analysis (IPA) and **c** GO Biological pathways from EnrichR analysis using the list of differentially expressed genes (adjusted p value < 0.05).

is highly expressed in the pig gallbladder and is necessary for gallbladder epithelial anion transport and fluid secretion. In addition, the CF pig gallbladder mucus phenotype is present at birth without significant alterations in mucin mRNA expression. Finding greater luminal MUC5AC and MUC5B accumulation in the newborn CF pig gallbladder suggests that these mucus changes are most likely due to defective fluid secretion and mucus clearance as opposed to mucin overproduction. Finally, these changes were associated with a limited number of alterations of transcriptional pathways in the CF pig gallbladder.

Our data suggest that CFTR plays an important role in gallbladder epithelial anion and liquid secretion. First, the gallbladder expresses a high level of CFTR. Single-cell RNA-sequencing and immunostaining demonstrated CFTR expression in nearly every gallbladder epithelial cell. Second, electrophysiological studies of excised gallbladder tissue revealed that the cAMP-mediated changes in I_{sc} are primarily CFTR-dependent. Forskolin-induced gallbladder fluid secretion was also CFTR-dependent in our organoid model. Earlier studies in human tissues have also found that CFTR contributes to anion transport in the gallbladder [19] and fluid secretion in murine gallbladder tissues [66]. We have previously shown that CFTR-mediated fluid secretion occurs during lung development [67]. Thus, in utero loss of CFTR-mediated fluid secretion might account for the micro-gallbladder present at birth in CF pigs. It is also possible that CFTR-mediated luminal anion secretion enables proper mucus secretion and clearance in the gallbladder. Finally, although we did not investigate this pathway, studies of intrahepatic bile duct units have found that CFTR might serve an additional role in cholangiocytes by contributing to ATP release [68].

Table 1 Bulk RNA-sequencing summary of gel-forming mucins for non-CF ($n = 4$) and CF ($n = 4$).

Mucin	non-CF TPM	CF TPM	Fold Change (CF/non-CF)	Adj. p value	95% CI
MUC2	0.68	5.86	8.36	0.15	(3.13, 22.35)
MUC5AC	83.16	139.40	1.39	0.81	(0.70, 2.77)
MUC5B	223.96	128.74	0.49	0.30	(0.29, 0.84)
MUC6	0.18	0.17	0.80	0.71	(0.44, 1.46)

TPM represents the mean of four animals per genotype from Kallisto. Fold change and confidence intervals are the product of DESeq2.

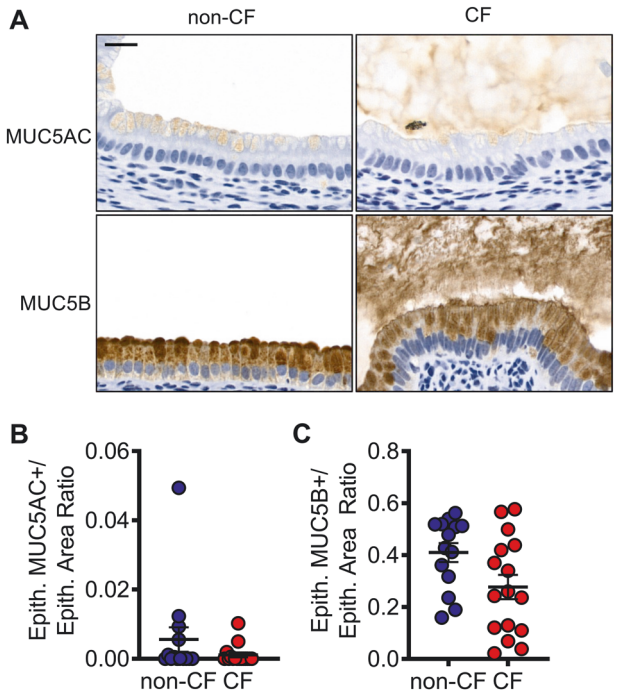

Fig. 6 Newborn CF pigs demonstrate mucus accumulation within the gallbladder lumen, but not in epithelium. a Mucin immunohistochemistry for non-CF and CF pig gallbladder tissue. Quantification of **b** MUC5AC and **c** MUC5B in the epithelium of newborn non-CF and CF pig gallbladders. Each symbol represents measurements from an individual animal. Bars represent mean ± SEM. Asterisk (*) indicates $p < 0.05$.

Table 2 Qualitative mucin immunohistochemistry of non-CF ($n = 11$) and CF ($n = 15$) gallbladder lumens.

Genotype	MUC5AC-positive luminal material	MUC5B-positive luminal material
non-CF	0% (0/11)	0% (0/11)
CF	60% (9/15)	100% (15/15)

Percentages and fractions (within parentheses) indicate the proportion of animals that have mucin-positive material in the gallbladder lumen.

Just as in humans with CF, CF pigs have microgallbladders [26] while other animal models, such as CF mice, have enlarged gallbladders [22]. Unlike pigs, however, microgallbladder occurs in only one-third of people with CF [13–16]. Gallbladder secretion may occur through cAMP-mediated and Ca^{2+}-mediated processes [19]. With loss of CFTR, mice may demonstrate increased activity in this latter mechanism whereas pigs do not have this compensatory response. Human biliary secretion may be a combination of cAMP- and Ca^{2+}-dependent mechanisms. This may explain the incomplete penetrance and variability of hepatobiliary disease in people with CF. However, studies indicate microgallbladder alone is not predicative of CF liver disease [7]. Other factors, such as mucus clearance, may be important in CF hepatobiliary disease.

CFTR loss in porcine gallbladder epithelium did not affect *MUC5AC* or *MUC5B* expression, but we did find increased MUC5AC and MUC5B accumulation in CF gallbladder lumens. In contrast, Kuver et al. found that mucin mRNA levels were reduced in murine CF gallbladder epithelial cells, while mucin secretion was increased [69]. Species differences and/or in vitro versus in vivo experimental models might account for differing findings.

It is interesting that nearly all epithelial cells in the porcine gallbladder express both CFTR and the gel-forming mucins MUC5AC and MUC5B. Whether this coexpression of CFTR and mucins in gallbladder epithelial cells is required for normal mucus secretion is not known. There is some evidence that CFTR is present on mucus granules in the gallbladder [70]. Similarly, CFTR is expressed in intestinal goblet cells and its loss leads to defective mucus release [71]. In contrast, studies in the airway show different cell types express CFTR and mucins [29, 72, 73]. Recently, a rare cell type in the airway, termed the ionocyte, has also been identified [74, 75]. The ionocyte is a Foxi1-positive cell which expresses very high levels of CFTR [74, 75]. While the function of the ionocyte is not clear, this discovery raises the question of whether a similar cell type exists in other epithelial tissues besides the lungs. Using single-cell RNA-sequencing, we did not find an "ionocyte-like" cell or any Foxi1-expressing cells in gallbladder epithelium. Future studies aimed at determining how CFTR expression is differentially regulated within the same and different tissues will be important in determining how loss of CFTR function in each of these cell types contributes to CF pathogenesis. At least in the gallbladder epithelium, our

data suggest that CFTR function in mucus secreting cells is essential to physiological mucus secretion and subsequent mucus clearance.

Reminiscent of the CF pig, gallbladder mucocele formation in domestic dogs also involves mucus obstruction of the gallbladder lumen. Kesimer et al. found that dogs with gallbladder mucoceles had increased MUC5AC and MUC5B content, an increased ratio of MUC5AC/MUC5B and defective mucin unpacking [76]. A subsequent metabolomics study found that dogs with gallbladder mucoceles had decreased levels of cAMP and adenosine, which could be associated with impaired CFTR-mediated fluid secretion and mucocele formation [77]. Similar to these findings, our study found decreased anion and fluid secretion with increased luminal mucus in the CF pig and further support an important role for CFTR in mucus clearance.

Our study found transcriptional alterations in several pathways. Mitochondrial-associated processes were enriched in both of our pathway analyses. Previous studies have found alterations in mitochondria physiology in CF including mitochondrial calcium uptake [78, 79], electron transport chain function [80–82], and reactive oxygen species generations [83]. The exact relationship between CFTR dysfunction and mitochondrial defects is unknown but could be an important focus for future studies. The NRF2-mediated oxidative stress response was also enriched in CF samples. Studies in the airway have found that CFTR loss associates with decreased NRF2 activity and increased oxidant levels [84]. Subsequent studies found that CFTR modulators rescue the Nrf2-associated phenotype in a CF mouse model [85] suggesting that NRF2 may play an important role in CF pathogenesis.

This study has strengths and limitations. Strengths include: (1) We use the CF pig, a model that recapitulates many aspects of CF disease seen in humans [24, 26, 28]. (2) The CF pig gallbladder demonstrates a mucus phenotype at birth in the absence of infection and consistent inflammation. This enabled our studies to be performed devoid of these confounding factors. (3) We investigated transcript-, protein-, and functional-level mechanisms that contribute to the mucus phenotype seen in the CF pig gallbladder. (4) We used a novel organoid model to assess fluid transport in the CF pig gallbladder epithelium. Limitations of this study include: (1) We did not assess real-time mucus secretion. While our histological studies suggest that the CF pig gallbladder epithelium can secrete but not clear mucus, we did not directly test this hypothesis. (2) We only studied the gallbladder at one timepoint. It would be informative to study the gallbladder phenotype at earlier time points in embryological development. (3) We did not examine how increased luminal mucus affects epithelial physiology in a chronic setting and how increased luminal mucus in the biliary tract contributes to CF hepatobiliary disease.

In conclusion, this study reveals mucus accumulation in the newborn CF pig gallbladder in the absence of infection or inflammation and without transcriptional changes in the gel-forming mucins. We also demonstrated fluid secretion defects in the CF gallbladder epithelium. These findings suggest that the CF pig gallbladder has defective mucus clearance and may have implications for initiation of CF hepatobiliary disease and future therapeutic approaches.

Acknowledgements We thank M. Abou Alaiwa, A. Comellas, H. de Jonge, M. Duffey, P. McCray, T. Moninger, F. Sampaziotis, M. Welsh, J. Zabner, the University of Iowa Office of Animal Resources, the University of Iowa Genomics Division, and the University of Iowa Comparative Pathology Lab for excellent assistance, advice, and discussions. This work was supported, in part, by NIH (HL091842, GM007337, and HL007638) and the Cystic Fibrosis Foundation (CFF Iowa Research Development Program).

Compliance with ethical standards

Conflict of interest The University of Iowa Research Foundation has licensed materials and technologies related to CF pigs to Exemplar Genetics. DAS is a coinventor of CF pigs.

References

1. Jackson AD, Goss CH. Epidemiology of CF: how registries can be used to advance our understanding of the CF population. J Cyst Fibros. 2018;17:297–305.
2. Welsh MJ, Ramsey BW, Accurso F, Cutting GR. Cystic fibrosis. In: Beaudet AL, Vogelstein B, Kinzler KW, et al. editors. The online metabolic and molecular bases of inherited disease. New York, NY: The McGraw-Hill Companies, Inc; 2014.
3. Colombo C, Battezzati PM, Crosignani A, Morabito A, Costantini D, Padoan R, et al. Liver disease in cystic fibrosis: a prospective study on incidence, risk factors, and outcome. Hepatology. 2002;36:1374–82.
4. Lamireau T, Monnereau S, Martin S, Marcotte JE, Winnock M, Alvarez F. Epidemiology of liver disease in cystic fibrosis: a longitudinal study. J Hepatol. 2004;41:920–5.
5. Scott-Jupp R, Lama M, Tanner MS. Prevalence of liver disease in cystic fibrosis. Arch Dis Child. 1991;66:698–701.
6. Bartlett JR, Friedman KJ, Ling SC, Pace RG, Bell SC, Bourke B, et al. Genetic modifiers of liver disease in cystic fibrosis. JAMA. 2009;302:1076–83.
7. Boelle PY, Debray D, Guillot L, Clement A, Corvol H, French CFMGSI. Cystic fibrosis liver disease: outcomes and risk factors in a large cohort of french patients. Hepatology. 2019;69:1648–56.
8. Toledano MB, Mukherjee SK, Howell J, Westaby D, Khan SA, Bilton D, et al. The emerging burden of liver disease in cystic fibrosis patients: a UK nationwide study. PLoS ONE. 2019;14:e0212779.
9. Waters DL, Dorney SF, Gruca MA, Martin HC, Howman-Giles R, Kan AE, et al. Hepatobiliary disease in cystic fibrosis patients with pancreatic sufficiency. Hepatology. 1995;21:963–9.
10. Kutney K, Donnola SB, Flask CA, Gubitosi-Klug R, O'Riordan M, McBennett K, et al. Lumacaftor/ivacaftor therapy is associated with reduced hepatic steatosis in cystic fibrosis patients. World J Hepatol. 2019;11:761–72.

11. Dray-Charier N, Paul A, Veissiere D, Mergey M, Scoazec JY, Capeau J, et al. Expression of cystic fibrosis transmembrane conductance regulator in human gallbladder epithelial cells. Lab Investig. 1995;73:828–36.
12. Moser AJ, Gangopadhyay A, Bradbury NA, Peters KW, Frizzell RA, Bridges RJ. Electrogenic bicarbonate secretion by prairie dog gallbladder. Am J Physiol Gastrointest Liver Physiol. 2007;292: G1683–94.
13. Assis DN, Debray D. Gallbladder and bile duct disease in cystic fibrosis. J Cyst Fibros. 2017;16(Suppl 2):S62–9.
14. Curry MP, Hegarty JE. The gallbladder and biliary tract in cystic fibrosis. Curr Gastroenterol Rep. 2005;7:147–53.
15. Nagel RA, Westaby D, Javaid A, Kavani J, Meire HB, Lombard MG, et al. Liver disease and bile duct abnormalities in adults with cystic fibrosis. Lancet. 1989;2:1422–5.
16. Rovsing H, Sloth K. Micro-gallbladder and biliary calculi in mucoviscidosis. Acta Radiol Diagn. 1973;14:588–92.
17. Uhlen M, Fagerberg L, Hallstrom BM, Lindskog C, Oksvold P, Mardinoglu A, et al. Proteomics. Tissue-based map of the human proteome. Science. 2015;347:1260419.
18. Strong TV, Boehm K, Collins FS. Localization of cystic fibrosis transmembrane conductance regulator mRNA in the human gastrointestinal tract by in situ hybridization. J Clin Investig. 1994;93:347–54.
19. Chinet T, Fouassier L, Dray-Charier N, Imam-Ghali M, Morel H, Mergey M, et al. Regulation of electrogenic anion secretion in normal and cystic fibrosis gallbladder mucosa. Hepatology. 1999;29:5–13.
20. Dray-Charier N, Paul A, Scoazec JY, Veissiere D, Mergey M, Capeau J, et al. Expression of delta F508 cystic fibrosis transmembrane conductance regulator protein and related chloride transport properties in the gallbladder epithelium from cystic fibrosis patients. Hepatology. 1999;29:1624–34.
21. Cuthbert AW. Bicarbonate secretion in the murine gallbladder–lessons for the treatment of cystic fibrosis. JOP. 2001;2: 257–62.
22. Debray D, Rainteau D, Barbu V, Rouahi M, El Mourabit H, Lerondel S, et al. Defects in gallbladder emptying and bile Acid homeostasis in mice with cystic fibrosis transmembrane conductance regulator deficiencies. Gastroenterology. 2012;142: 1581–91. e1586
23. Bodewes FA, Bijvelds MJ, de Vries W, Baller JF, Gouw AS, de Jonge HR, et al. Cholic acid induces a Cftr dependent biliary secretion and liver growth response in mice. PLoS ONE. 2015;10: e0117599.
24. Rogers CS, Stoltz DA, Meyerholz DK, Ostedgaard LS, Rokhlina T, Taft PJ, et al. Disruption of the CFTR gene produces a model of cystic fibrosis in newborn pigs. Science. 2008;321:1837–41.
25. Stoltz DA, Meyerholz DK, Welsh MJ. Origins of cystic fibrosis lung disease. N Engl J Med. 2015;372:351–62.
26. Meyerholz DK, Stoltz DA, Pezzulo AA, Welsh MJ. Pathology of gastrointestinal organs in a porcine model of cystic fibrosis. Am J Pathol. 2010;176:1377–89.
27. Uc A, Giriyappa R, Meyerholz DK, Griffin M, Ostedgaard LS, Tang XX, et al. Pancreatic and biliary secretion are both altered in cystic fibrosis pigs. Am J Physiol Gastrointest Liver Physiol. 2012;303:G961–8.
28. Stoltz DA, Meyerholz DK, Pezzulo AA, Ramachandran S, Rogan MP, Davis GJ, et al. Cystic fibrosis pigs develop lung disease and exhibit defective bacterial eradication at birth. Sci Transl Med. 2010;2:29ra31.
29. Meyerholz DK, Lambertz AM, Reznikov LR, Ofori-Amanfo GK, Karp PH, McCray PB Jr., et al. Immunohistochemical detection of markers for translational studies of lung disease in pigs and humans. Toxicol Pathol. 2016;44:434–41.
30. Chen JH, Stoltz DA, Karp PH, Ernst SE, Pezzulo AA, Moninger TO, et al. Loss of anion transport without increased sodium absorption characterizes newborn porcine cystic fibrosis airway epithelia. Cell. 2010;143:911–23.
31. Sampaziotis F, Justin AW, Tysoe OC, Sawiak S, Godfrey EM, Upponi SS, et al. Reconstruction of the mouse extrahepatic biliary tree using primary human extrahepatic cholangiocyte organoids. Nat Med. 2017;23:954–63.
32. Bray NL, Pimentel H, Melsted P, Pachter L. Near-optimal probabilistic RNA-seq quantification. Nat Biotechnol. 2016;34:525–7.
33. Pimentel H, Bray NL, Puente S, Melsted P, Pachter L. Differential analysis of RNA-seq incorporating quantification uncertainty. Nat Methods. 2017;14:687–90.
34. Love MI, Huber W, Anders S. Moderated estimation of fold change and dispersion for RNA-seq data with DESeq2. Genome Biol. 2014;15:550.
35. Chen EY, Tan CM, Kou Y, Duan Q, Wang Z, Meirelles GV, et al. Enrichr: interactive and collaborative HTML5 gene list enrichment analysis tool. BMC Bioinformatics. 2013;14:128.
36. Kuleshov MV, Jones MR, Rouillard AD, Fernandez NF, Duan Q, Wang Z, et al. Enrichr: a comprehensive gene set enrichment analysis web server 2016 update. Nucleic Acids Res. 2016;44:W90–7.
37. Dobin A, Davis CA, Schlesinger F, Drenkow J, Zaleski C, Jha S, et al. STAR: ultrafast universal RNA-seq aligner. Bioinformatics. 2013;29:15–21.
38. Butler A, Hoffman P, Smibert P, Papalexi E, Satija R. Integrating single-cell transcriptomic data across different conditions, technologies, and species. Nat Biotechnol. 2018;36:411–20.
39. Stuart T, Butler A, Hoffman P, Hafemeister C, Papalexi E, Mauck WM 3rd, et al. Comprehensive integration of single-cell data. Cell. 2019;177:1888–902. e1821
40. Cohn JA, Strong TV, Picciotto MR, Nairn AC, Collins FS, Fitz JG. Localization of the cystic fibrosis transmembrane conductance regulator in human bile duct epithelial cells. Gastroenterology. 1993;105:1857–64.
41. Pezzulo AA, Tang XX, Hoegger MJ, Abou Alaiwa MH, Ramachandran S, Moninger TO, et al. Reduced airway surface pH impairs bacterial killing in the porcine cystic fibrosis lung. Nature. 2012;487:109–13.
42. Shah VS, Ernst S, Tang XX, Karp PH, Parker CP, Ostedgaard LS, et al. Relationships among CFTR expression, HCO3- secretion, and host defense may inform gene- and cell-based cystic fibrosis therapies. Proc Natl Acad Sci USA. 2016;113:5382–7.
43. Joo NS, Cho HJ, Khansaheb M, Wine JJ. Hyposecretion of fluid from tracheal submucosal glands of CFTR-deficient pigs. J Clin Investig. 2010;120:3161–6.
44. Hoegger MJ, Fischer AJ, McMenimen JD, Ostedgaard LS, Tucker AJ, Awadalla MA, et al. Impaired mucus detachment disrupts mucociliary transport in a piglet model of cystic fibrosis. Science. 2014;345:818–22.
45. Clarke LL, Stien X, Walker NM. Intestinal bicarbonate secretion in cystic fibrosis mice. JOP. 2001;2:263–7.
46. Gustafsson JK, Ermund A, Ambort D, Johansson ME, Nilsson HE, Thorell K, et al. Bicarbonate and functional CFTR channel are required for proper mucin secretion and link cystic fibrosis with its mucus phenotype. J Exp Med. 2012;209:1263–72.
47. Birket SE, Davis JM, Fernandez CM, Tuggle KL, Oden AM, Chu KK, et al. Development of an airway mucus defect in the cystic fibrosis rat. JCI Insight. 2018;3:e97199.
48. Yang N, Garcia MA, Quinton PM. Normal mucus formation requires cAMP-dependent HCO3- secretion and Ca2+-mediated mucin exocytosis. J Physiol. 2013;591:4581–93.
49. Quinton PM. The neglected ion: HCO3. Nat Med. 2001;7:292–3.
50. van Klinken BJ, Dekker J, van Gool SA, van Marle J, Buller HA, Einerhand AW. MUC5B is the prominent mucin in human

gallbladder and is also expressed in a subset of colonic goblet cells. Am J Physiol. 1998;274:G871–8.
51. Vandenhaute B, Buisine MP, Debailleul V, Clement B, Moniaux N, Dieu MC, et al. Mucin gene expression in biliary epithelial cells. J Hepatol. 1997;27:1057–66.
52. Reid CJ, Hyde K, Ho SB, Harris A. Cystic fibrosis of the pancreas: involvement of MUC6 mucin in obstruction of pancreatic ducts. Mol Med. 1997;3:403–11.
53. Sasaki M, Ikeda H, Nakanuma Y. Expression profiles of MUC mucins and trefoil factor family (TFF) peptides in the intrahepatic biliary system: physiological distribution and pathological significance. Prog Histochem Cytochem. 2007;42:61–110.
54. Dutta AK, Khimji AK, Kresge C, Bugde A, Dougherty M, Esser V, et al. Identification and functional characterization of TMEM16A, a Ca2+-activated Cl- channel activated by extracellular nucleotides, in biliary epithelium. J Biol Chem. 2011; 286:766–76.
55. Marinelli RA, Tietz PS, Pham LD, Rueckert L, Agre P, LaRusso NF. Secretin induces the apical insertion of aquaporin-1 water channels in rat cholangiocytes. Am J Physiol. 1999;276: G280–286.
56. Banales JM, Arenas F, Rodriguez-Ortigosa CM, Saez E, Uriarte I, Doctor RB, et al. Bicarbonate-rich choleresis induced by secretin in normal rat is taurocholate-dependent and involves AE2 anion exchanger. Hepatology. 2006;43:266–75.
57. Mennone A, Biemesderfer D, Negoianu D, Yang CL, Abbiati T, Schultheis PJ, et al. Role of sodium/hydrogen exchanger isoform NHE3 in fluid secretion and absorption in mouse and rat cholangiocytes. Am J Physiol Gastrointest Liver Physiol. 2001;280: G247–54.
58. Fiorotto R, Scirpo R, Trauner M, Fabris L, Hoque R, Spirli C, et al. Loss of CFTR affects biliary epithelium innate immunity and causes TLR4-NF-kappaB-mediated inflammatory response in mice. Gastroenterology. 2011;141:1498–508.
59. Wang AP, Migita K, Ito M, Takii Y, Daikoku M, Yokoyama T, et al. Hepatic expression of toll-like receptor 4 in primary biliary cirrhosis. J Autoimmun. 2005;25:85–91.
60. Cho WK, Boyer JL. Vasoactive intestinal polypeptide is a potent regulator of bile secretion from rat cholangiocytes. Gastroenterology. 1999;117:420–8.
61. Korner M, Hayes GM, Rehmann R, Zimmermann A, Scholz A, Wiedenmann B, et al. Secretin receptors in the human liver: expression in biliary tract and cholangiocarcinoma, but not in hepatocytes or hepatocellular carcinoma. J Hepatol. 2006;45: 825–35.
62. Donner MG, Keppler D. Up-regulation of basolateral multidrug resistance protein 3 (Mrp3) in cholestatic rat liver. Hepatology. 2001;34:351–9.
63. Soroka CJ, Ballatori N, Boyer JL. Organic solute transporter, OSTalpha-OSTbeta: its role in bile acid transport and cholestasis. Semin Liver Dis. 2010;30:178–85.
64. Soroka CJ, Mennone A, Hagey LR, Ballatori N, Boyer JL. Mouse organic solute transporter alpha deficiency enhances renal excretion of bile acids and attenuates cholestasis. Hepatology. 2010;51:181–90.
65. Tabibian JH, Masyuk AI, Masyuk TV, O'Hara SP, LaRusso NF. Physiology of cholangiocytes. Compr Physiol. 2013;3:541–65.
66. Peters RH, van Doorninck JH, French PJ, Ratcliff R, Evans MJ, Colledge WH, et al. Cystic fibrosis transmembrane conductance regulator mediates the cyclic adenosine monophosphate-induced fluid secretion but not the inhibition of resorption in mouse gallbladder epithelium. Hepatology. 1997;25:270–7.
67. Meyerholz DK, Stoltz DA, Gansemer ND, Ernst SE, Cook DP, Strub MD, et al. Lack of cystic fibrosis transmembrane conductance regulator disrupts fetal airway development in pigs. Lab Investig. 2018;98:825–38.
68. Minagawa N, Nagata J, Shibao K, Masyuk AI, Gomes DA, Rodrigues MA, et al. Cyclic AMP regulates bicarbonate secretion in cholangiocytes through release of ATP into bile. Gastroenterology. 2007;133:1592–602.
69. Kuver R, Wong T, Klinkspoor JH, Lee SP. Absence of CFTR is associated with pleiotropic effects on mucins in mouse gallbladder epithelial cells. Am J Physiol Gastrointest Liver Physiol. 2006;291:G1148–54.
70. Kuver R, Klinkspoor JH, Osborne WR, Lee SP. Mucous granule exocytosis and CFTR expression in gallbladder epithelium. Glycobiology. 2000;10:149–57.
71. Liu J, Walker NM, Ootani A, Strubberg AM, Clarke LL. Defective goblet cell exocytosis contributes to murine cystic fibrosis-associated intestinal disease. J Clin Investig. 2015;125:1056–68.
72. Kreda SM, Mall M, Mengos A, Rochelle L, Yankaskas J, Riordan JR, et al. Characterization of wild-type and deltaF508 cystic fibrosis transmembrane regulator in human respiratory epithelia. Mol Biol Cell. 2005;16:2154–67.
73. Wu JV, Krouse ME, Wine JJ. Acinar origin of CFTR-dependent airway submucosal gland fluid secretion. Am J Physiol Lung Cell Mol Physiol. 2007;292:L304–11.
74. Montoro DT, Haber AL, Biton M, Vinarsky V, Lin B, Birket SE, et al. A revised airway epithelial hierarchy includes CFTR-expressing ionocytes. Nature. 2018;560:319–24.
75. Plasschaert LW, Zilionis R, Choo-Wing R, Savova V, Knehr J, Roma G, et al. A single-cell atlas of the airway epithelium reveals the CFTR-rich pulmonary ionocyte. Nature. 2018;560:377–81.
76. Kesimer M, Cullen J, Cao R, Radicioni G, Mathews KG, Seiler G, et al. Excess secretion of gel-forming mucins and associated innate defense proteins with defective mucin un-packaging underpin gallbladder mucocele formation in dogs. PLoS ONE. 2015;10:e0138988.
77. Gookin JL, Mathews KG, Cullen J, Seiler G. Qualitative metabolomics profiling of serum and bile from dogs with gallbladder mucocele formation. PLoS ONE. 2018;13:e0191076.
78. Feigal RJ, Shapiro BL. Mitochondrial calcium uptake and oxygen consumption in cystic fibrosis. Nature. 1979;278:276–7.
79. Antigny F, Girardin N, Raveau D, Frieden M, Becq F, Vandebrouck C. Dysfunction of mitochondria Ca2+ uptake in cystic fibrosis airway epithelial cells. Mitochondrion. 2009;9:232–41.
80. Shapiro BL, Feigal RJ, Lam LF. Mitrochondrial NADH dehydrogenase in cystic fibrosis. Proc Natl Acad Sci USA. 1979;76:2979–83.
81. Shapiro BL, Lam LF, Feigal RJ. Mitochondrial NADH dehydrogenase in cystic fibrosis: enzyme kinetics in cultured fibroblasts. Am J Hum Genet. 1982;34:846–52.
82. Kelly-Aubert M, Trudel S, Fritsch J, Nguyen-Khoa T, Baudouin-Legros M, Moriceau S, et al. GSH monoethyl ester rescues mitochondrial defects in cystic fibrosis models. Hum Mol Genet. 2011;20:2745–59.
83. Atlante A, Favia M, Bobba A, Guerra L, Casavola V, Reshkin SJ. Characterization of mitochondrial function in cells with impaired cystic fibrosis transmembrane conductance regulator (CFTR) function. J Bioenerg Biomembr. 2016;48:197–210.
84. Chen J, Kinter M, Shank S, Cotton C, Kelley TJ, Ziady AG. Dysfunction of Nrf-2 in CF epithelia leads to excess intracellular H2O2 and inflammatory cytokine production. PLoS ONE. 2008;3: e3367.
85. Borcherding DC, Siefert ME, Lin S, Brewington J, Sadek H, Clancy JP, et al. Clinically-approved CFTR modulators rescue Nrf2 dysfunction in cystic fibrosis airway epithelia. J Clin Investig. 2019;129:3448–63.